Published OnlineFirst March 27, 2012; DOI: 10.1158/1078-0432.CCR-11-1078

Human Cancer Biology

Clinical Cancer Research

Microarray Analysis of Colorectal Cancer Stromal Tissue Reveals Upregulation of Two Oncogenic miRNA Clusters

Naohiro Nishida[1,4], Makoto Nagahara[2], Tetsuya Sato[3], Koshi Mimori[1], Tomoya Sudo[1], Fumiaki Tanaka[1], Kohei Shibata[1], Hideshi Ishii[1,4], Kenichi Sugihara[2], Yuichiro Doki[4], and Masaki Mori[1,4]

Abstract

Purpose: Cancer stroma plays an important role in the progression of cancer. Although alterations in miRNA expression have been explored in various kinds of cancers, the expression of miRNAs in cancer stroma has not been explored in detail.

Experimental Design: Using a laser microdissection technique, we collected RNA samples specific for epithelium or stroma from 13 colorectal cancer tissues and four normal tissues, and miRNA microarray and gene expression microarray were carried out. The expression status of miRNAs was confirmed by reverse transcriptase PCR. Furthermore, we investigated whether miRNA expression status in stromal tissue could influence the clinicopathologic factors.

Results: Oncogenic miRNAs, including two miRNA clusters, *miR-17-92a* and *miR-106b-25* cluster, were upregulated in cancer stromal tissues compared with normal stroma. Gene expression profiles from cDNA microarray analyses of the same stromal tissue samples revealed that putative targets of these miRNA clusters, predicted by Target Scan, such as *TGFBR2*, *SMAD2*, and *BMP* family genes, were significantly downregulated in cancer stromal tissue. Downregulated putative targets were also found to be involved in cytokine interaction and cellular adhesion. Importantly, expression of miR-25 and miR-92a in stromal tissues was associated with a variety of clinicopathologic factors.

Conclusions: Oncogenic miRNAs were highly expressed in cancer stroma. Although further validation is required, the finding that stromal miRNA expression levels were associated with clinicopathologic factors suggests the possibility that miRNAs in cancer stroma are crucially involved in cancer progression. *Clin Cancer Res; 18(11); 1–17. ©2012 AACR.*

Introduction

Cancer tissues consist of cancer cells and surrounding stromal cells, including inflammatory cells, immunocompetent cells, endothelial cells, and fibroblasts. Cancer stroma interacts with cancer tissues directly or indirectly through cytokines, creating a niche for the cancer cells. Recent studies have focused on altered expression of oncogenes and tumor suppressor genes in stromal tissues. Kurose and colleagues reported that the downregulation of PTEN and p53 is a key step in breast cancer progression, and other reports have indicated that ablation of TGFBR2 in fibroblasts can lead to carcinogenesis *in vivo* (1–3).

With regard to clinical aspects, a number of studies have revealed the gene expression status of cancer stroma and its correlation to prognosis as well as clinicopathologic factors (4, 5). Particularly, Finak and colleagues analyzed global gene expression patterns in breast cancer stromal tissues and identified gene sets that potently influenced prognosis (6). They revealed that the aggressiveness of cancer could be defined by gene expression patterns in stromal tissue. Moreover, Fukino and colleagues revealed that cancer-specific LOH or allelic imbalance in stromal cells is more highly correlated with clinicopathologic features than that in epithelial cells (7). These findings suggest that cancer stromal tissues are actively involved in cancer progression.

miRNAs constitute a class of small (19–25 nucleotides) noncoding RNAs that function as posttranscriptional gene regulators by binding to their target mRNAs (8). Alterations in miRNA expression are reported in various kinds of human cancers, suggesting miRNAs function both as tumor suppressors and oncogenes in cancer development (9). Genetic alterations in cancer tissues are likely dependent largely on the expression status of miRNAs (9). We

Authors' Affiliations: [1]Department of Surgery and Molecular Oncology, Medical Institute of Bioregulation, Kyushu University, Oita; [2]Department of Surgical Oncology, Tokyo Medical and Dental University, Graduate School of Medical & Dental Science, Tokyo; [3]Center for Genomic Medicine, Kyoto University Graduate School of Medicine, Kyoto; and [4]Department of Gastroenterological Surgery, Osaka University Graduate School of Medicine, Osaka, Japan

Note: Supplementary data for this article are available at Clinical Cancer Research Online (http://clincancerres.aacrjournals.org/).

Corresponding Author: Masaki Mori, Department of Gastroenterological Surgery, Osaka University Graduate School of Medicine, 2-2 Yamada-oka, Suita City, Osaka 565-0871, Japan. Phone: 81-6-6879-3251; Fax: 81-6-6879-3259; E-mail: mmori@gesurg.med.osaka-u.ac.jp

doi: 10.1158/1078-0432.CCR-11-1078

Published OnlineFirst March 27, 2012; DOI: 10.1158/1078-0432.CCR-11-1078

Translational Relevance

Cancer stroma plays a critical role in cancer progression. To investigate the role of miRNAs in colorectal cancer stroma, we carried out epithelial and stromal tissue-specific miRNA microarray analyses using a laser microdissection technique. We found that oncogenic miRNAs, including the *miR-17-92a* cluster and the *miR-106b-25* cluster, which are known to be involved in cancer progression in epithelial tissue, were significantly upregulated in cancer stromal tissue compared with normal stroma. Gene expression profiles from cDNA microarray analyses of the same stromal tissue samples revealed that putative targets of these miRNA clusters, predicted by TargetScan, such as *TGFBR2*, *SMAD2*, and *BMP* family genes, were significantly downregulated in cancer stromal tissue. Furthermore, miRNA expression in colorectal cancer stroma was associated with a number of clinicopathologic factors. Although further validation is required, these findings suggest the possibility that miRNAs in stromal tissues are functionally associated with cancer progression.

considered the possibility that gene expression in cancer stroma is also regulated by miRNAs expressed in cancer stroma.

Conventional gene expression analysis using bulk tumor samples could not reveal the gene and miRNA expression profiles in cancer stroma. In this study, using a laser microdissection (LMD) method, we collected epithelium-specific and stoma-specific RNAs, and investigated the miRNA and gene expression profiles. By analyzing many kinds of microarray data, including that of epithelium, stroma, normal, and cancer, we show how miRNAs in cancer stroma are involved in cancer progression.

Materials and Methods

Clinical samples

Tissues from 13 cases of colorectal cancer and 4 normal colorectal tissues (located more than 5 cm from the colorectal cancer) were obtained during surgery. All patients underwent resection of the primary tumor at Kyushu University Hospital at Beppu and affiliated hospitals between 1993 and 2006. Written informed consent was obtained from all patients, and the study protocol was approved by the local ethics committee. Detailed information is described in Supplementary Data.

Laser microdissection

Tissue samples were microdissected using the LMD system LMD6000 (Leica Laser Microdissection System; Leica Microsystems) as previously described (10). Detailed protocols are described in Supplementary Information.

To show the accuracy of LMD and RNA separation, we presented tissue section before (left) and after (right) LMD in 6 representative samples of colorectal cancer (Supplementary Fig. S1).

miRNA microarray

Total RNAs from epithelial and stromal tissues of cancer and normal samples were analyzed by miRNA microarray. Total RNA was extracted from tissue using the miRNeasy Mini Kit (Qiagen) according to the manufacturer's protocol. Concentrations and purities of the total RNAs were assessed with a spectrophotometer and RNA integrity was verified using an Agilent 2100 Bioanalyzer (Agilent Technologies). OD_{260}/OD_{280} ratios of 1.8 to 2.1 were accepted to be adequate for microarray. Total RNA (100 ng) was directly labeled with cyanine 3-CTP (Cy3), without fractionation or amplification, using an Agilent protocol that produces precise and accurate measurements spanning a linear dynamic range from 0.2 amol to 2 fmol of input miRNA. Each total RNA sample (100 ng) was competitively hybridized to a miRNA array (Agilent Microarray Design ID = 014947, Early Access version) containing 455 miRNAs [version 15 of the Sanger miRNA database (http://www.mirbase.org/)], according to the manufacturer's protocol (11). The intensity of each hybridization signal was evaluated using Extraction Software Version A.7.5.1 (Agilent Technologies), which used the locally weighted linear regression curve fit (LOWESS) normalization method (12).The robust multiarray average algorithm normalization method was also used for analysis in downregulated miRNAs in cancer stroma (13, 14). miRNA arrays have been deposited in the National Center for Biotechnology Information (NCBI) Gene Expression Omnibus (GEO) database with accession code GSE35602.

cDNA microarray

We used the commercially available Human Whole Genome Oligo DNA Microarray Kit (Agilent Technologies). A list of genes on this cDNA microarray is available from http://www.chem.agilent.com. Cyanine (Cy)-labeled cRNA was prepared using T7 linear amplification as described in the Agilent Low RNA Input Fluorescent Linear Amplification Kit Manual (Agilent Technologies). Labeled cRNA was fragmented and hybridized to an oligonucleotide microarray (Whole Human Genome 4 × 44 K Agilent G4112F). Fluorescence intensities were determined with an Agilent DNA Microarray Scanner and were analyzed using G2567AA Feature Extraction Software Version A.7.5.1 (Agilent Technologies), which used the LOWESS normalization method (12). This microarray study followed MIAME guidelines issued by the Microarray Gene Expression Data group (15). Gene expression arrays have been deposited in the NCBI GEO database with accession code GSE35602.

Gene ontology analysis and miRNA target prediction

A total of 1,939 Gene set enrichment analyses of differentially expressed genes were carried out using Gene Codis version 2.0 (16, 17). The Kyoto Encyclopedia of Genes and

Published OnlineFirst March 27, 2012; DOI: 10.1158/1078-0432.CCR-11-1078

Genomes (KEGG) database (18) was used for systematic analysis of gene functions. TargetScan (19, 20) Version 5.1 algorithm was used to predict putative targets of each miRNA. TargetScan focuses on the exact match to 7 bases or more (hexamer match in positions 2–7, plus an adenosine at a position on the 3′ side) of the miRNA seed sequence in the 3′-untranslated region of target messenger RNA. In our analysis, we included all targets that met TargetScan criteria without taking into account evolutionary conservation.

Quantitative real-time reverse transcriptase PCR

For *miR-25* and *miR-92a* quantitative real-time reverse transcriptase PCR (qRT-PCR), cDNA was synthesized from 10 ng of total RNA using TaqMan miRNA hsa-*miR-25*- or *92a*-specific primers (Applied Biosystems) and a TaqMan MicroRNA Reverse Transcription Kit (Applied Biosystems). RT-PCR protocols are described in Supplementary Information.

Statistical analysis

Differences between groups were estimated using the χ^2 test and Student *t* test. After expression signals were calculated by $\log_2$ transformation of the normalized data, differentially expressed miRNAs and genes were detected by using the fold-change value and *Q* value. We used the significance analysis of microarrays method in the "samr" package of the R language (http://www.r-project.org/). RT-PCR data were analyzed using JMP software (SAS Institute Inc.). All differences were considered statistically significant at the level of $P < 0.05$ or $Q < 0.05$.

Results

The miR-17-92a cluster and miR-106b-25 cluster were upregulated in cancer stroma compared with normal stroma

To investigate the functions of miRNAs in cancer stroma, we carried out miRNA microarray analyses with samples of 13 cancer stromal tissue and 4 samples of normal stromal tissue. Those miRNAs that were significantly upregulated in cancer stromal tissues compared with normal stromal tissues are listed in Table 1 (fold change >1.5, and $Q < 0.05$). For example, oncogenic miRNAs, including *miR-21*, *miR-221*, and almost all components of the oncogenic *miR-17-92a* cluster and *miR-106b-25* cluster except *miR-19b* were upregulated in cancer stromal tissue compared with normal stromal tissue (Table 1). Unsupervised hierarchical clustering of normal and cancerous stromal samples revealed that all components of the *miR-17-92a* cluster and the *miR-106b-25* cluster (except for *miR-92a*) were classified in the same cluster (Supplementary Fig. S2A and S2B). *MiR-92a* was classified in another cluster, perhaps because *miR-92a* has a homolog (*miR-92a-2*) on chromosome X, besides *miR-92a-1* in the miRNA cluster on chromosome 13 (21). Therefore, its expression could have diverged from the expression of other miRNAs in the cluster.

The correlation coefficient ratio was significantly higher within miRNA clusters (Supplementary Table S1). These clusters are transcribed from another chromosome. The *miR-17-92a* cluster was located on chromosome 13 in the host gene *C13ORF25*, and its homolog *miR-106b-25* cluster was located in the intron of the host gene MCM7 on chromosome 7 (Fig. 1, top part). Some components shared the same seed sequence (Fig. 1, bottom part), suggesting they regulated the same targets simultaneously.

In 4 of the 13 samples of cancer tissue and the 4 normal tissues, both epithelial and stromal samples were available. Thus, we carried out combined analyses in epithelial and stromal tissues in these samples. The expression status of epithelial tissues was highly correlated with that of stromal tissues, and the expression of miRNA in the epithelium was always higher than that in the stroma in all components of the *miR-17-92a* cluster and the *miR-106b-25* cluster (Fig. 2).

Significantly downregulated genes which are putative targets of the miR-17-92a and miR-106b-25 clusters are involved in a variety of cellular functions

We also carried out gene expression array analyses using the same samples used in the miRNA microarray. We identified significantly downregulated genes (fold change < 0.5 and $Q < 0.05$), which were putative targets of the *miR-17-92a* and *miR-106b-25* clusters. The number of genes that matched these criteria was 1,939. Gene set enrichment analysis using Gene Codis version 2.0 (16, 17) and KEGG revealed that the following molecules were enriched: KEGG 04060: cytokine–cytokine receptor interaction [chemokines, hematopoietins, platelet-derived growth factor (PDGF) family, TNF family, and TGFβ family], KEGG 04340: hedgehog signaling pathway, KEGG 05200: pathways in cancer, and KEGG 04514: cell adhesion molecules (CAM; Table 2, Supplementary Table S2A). These indicated the possibility that the *miR-17-92a* and *miR-25-106b* clusters were involved in those important pathways in colorectal cancer stroma.

Identification of a putative miRNA gene pathway focusing on inverse correlations between miRNAs and genes

We used different approaches to identify putative targets of the *miR-17-92a* and *miR-106b-25* clusters. Combining the microarray data of miRNAs and genes in stromal samples, we identified highly inversely correlated miRNA gene pairs, which were putative pathways predicted by TargetScan (refs. 19, 20; correlation coefficient >0.65 and $P < 0.05$; Table 3). These included a number of crucial regulators of cellular function, such as the apoptosis-related *miR-17* death–associated protein kinase 2 (*DAPK*) pairing, the *miR-18a*–caspase 7 pairing, and the *miR-17* cancer-related transcription factor 7 (*TCF7*) pairing.

miR-25 and miR-92a expression status in colorectal cancer stromal tissue

The miRNA array analysis revealed that 2 oncogenic miRNA clusters were upregulated in colorectal cancer stroma. Therefore, we confirmed the expression status of 2

Published OnlineFirst March 27, 2012; DOI: 10.1158/1078-0432.CCR-11-1078

Table 1. Upregulated miRNAs in colorectal cancer stromal tissue compared with normal stromal tissue

Systematic name	Signal in cancer stromal tissue (log_2)	Signal in normal stromal tissue (log_2)	Fold change	*Q* (%)
hsa-miR-214	7.3612	5.1633	4.5882	0.0000
hsa-miR-21	13.7414	11.7651	3.9348	0.0000
hsa-miR-455-3p	5.0351	3.4322	3.0376	0.0000
hsa-miR-663	4.4278	2.7578	3.1820	0.0000
hsa-miR-127-3p	3.7355	1.9303	3.4947	0.0000
hsa-miR-92a	7.2865	5.7584	2.8842	0.0000
hsa-miR-381	3.9035	2.5478	2.5593	0.0000
hsa-miR-93	5.5042	4.0246	2.7886	0.0000
hsa-miR-224	4.5767	2.2308	5.0840	0.0000
hsa-miR-432	2.6401	1.3709	2.4102	0.0000
hsa-miR-221	5.1187	3.6628	2.7433	0.0000
hsa-miR-125b	7.7959	5.7433	4.1486	0.0000
hsa-miR-17	6.3813	4.9449	2.7064	0.0000
hsa-miR-337-5p	2.8150	1.4391	2.5952	0.0000
hsa-miR-502-3p	1.8047	0.5097	2.4538	0.0000
hsa-miR-300	3.6767	2.3557	2.4985	0.0000
hsa-miR-128	2.5359	1.3263	2.3127	0.0000
hsa-miR-532-5p	2.7469	1.5402	2.3080	0.0000
hsa-miR-609	3.8840	2.8980	1.9806	0.0000
hsa-miR-130b	4.1915	2.7904	2.6409	0.0000
hsa-miR-18a	3.7635	1.3688	5.2588	0.0000
hsa-miR-181d	3.1301	2.0477	2.1175	0.0000
hsa-miR-362-5p	3.2330	2.0853	2.2156	0.0000
hsa-miR-424	7.7230	5.9653	3.3816	0.0000
hsa-miR-152	3.1990	1.6066	3.0156	0.0000
hsa-miR-654-3p	4.3411	2.6129	3.3130	0.0000
hsa-miR-149	3.8869	2.7086	2.2632	0.0000
hsa-miR-7	4.7678	2.8344	3.8196	0.0000
hsa-miR-485-3p	5.3006	4.2385	2.0880	0.0000
hsa-miR-99b	3.9191	2.6203	2.4603	0.0000
hsa-miR-933	2.7300	1.7161	2.0193	0.0000
hsa-miR-615-3p	3.8335	2.6442	2.2804	0.0000
hsa-miR-640	2.9456	1.4328	2.8535	0.0000
hsa-miR-483-3p	6.2669	5.0075	2.3940	0.0000
hsa-miR-605	3.8121	2.5917	2.3301	0.0000
hsa-miR-135b	3.8255	0.7653	8.3408	0.0000
hsa-miR-296-5p	1.9389	1.1457	1.7329	0.0000
hsa-miR-647	3.8730	2.1903	3.2102	0.0000
hsa-miR-1236	3.4103	1.8925	2.8635	0.0000
hsa-miR-34b	4.2683	2.3956	3.6620	0.0000
hsa-miR-592	2.5548	0.8012	3.3721	0.4839
hsa-miR-25	5.9887	4.7911	2.2936	0.4839
hsa-let-7i	8.6952	7.6400	2.0781	0.4839
hsa-miR-20b	5.5041	4.2857	2.3269	0.4839
hsa-miR-130a	7.3585	6.0856	2.4165	0.4839
hsa-miR-199a-5p	7.4083	5.9666	2.7163	0.4839
hsa-miR-1238	4.2775	3.5734	1.6291	0.4839
hsa-miR-331-3p	6.6993	5.5074	2.2846	0.4839
hsa-miR-24	9.5984	8.5492	2.0693	0.4839
hsa-miR-20a	7.5321	6.3601	2.2532	0.4839
hsa-miR-23a	10.0837	9.0655	2.0254	0.4839
hsa-miR-199b-5p	6.7800	5.3520	2.6907	0.4839
hsa-miR-181b	4.6692	3.7467	1.8955	0.4839

(Continued on the following page)

Published OnlineFirst March 27, 2012; DOI: 10.1158/1078-0432.CCR-11-1078

Table 1. Upregulated miRNAs in colorectal cancer stromal tissue compared with normal stromal tissue (Cont'd)

Systematic name	Signal in cancer stromal tissue (log_2)	Signal in normal stromal tissue (log_2)	Fold change	*Q* (%)
hsa-miR-377	4.4965	3.2165	2.4283	0.4839
hsa-miR-18b	2.5247	0.9391	3.0013	0.4839
hsa-miR-539	2.0809	1.0446	2.0510	0.4839
hsa-miR-22	9.7884	8.6262	2.2379	0.4839
hsa-miR-223	8.8473	7.7969	2.0712	0.4839
hsa-miR-491-3p	2.5471	0.9916	2.9393	0.4839
hsa-miR-125a-5p	5.6168	4.5834	2.0469	0.4839
hsa-miR-299-5p	3.1356	1.7790	2.5607	0.4839
hsa-miR-483-5p	4.9531	3.9757	1.9689	0.4839
hsa-miR-379	2.4551	0.4574	3.9938	0.4839
hsa-miR-1234	5.0701	4.3136	1.6894	0.4839
hsa-miR-99a	3.9888	2.3726	3.0657	0.4839
hsa-miR-1225-3p	3.9937	3.3510	1.5613	0.4839
hsa-miR-495	2.3389	0.7363	3.0369	0.4839
hsa-miR-574-5p	7.1083	6.2371	1.8292	0.4839
hsa-miR-125a-3p	3.2257	2.3094	1.8873	0.4839
hsa-miR-326	1.9496	0.8913	2.0825	0.4839
hsa-miR-1224-3p	4.8757	3.6868	2.2798	0.4839
hsa-miR-1229	3.7613	2.5318	2.3448	0.4839
hsa-miR-937	4.9785	3.8112	2.2459	0.4839
hsa-miR-574-3p	7.9370	7.0906	1.7979	0.4839
hsa-miR-1237	2.8475	2.0403	1.7498	0.4839
hsa-miR-206	3.0294	1.7743	2.3868	0.4839
hsa-miR-129-3p	1.7338	0.7030	2.0432	0.4839
hsa-miR-885-5p	6.2987	5.1769	2.1761	0.4839
hsa-miR-1227	4.6286	3.0407	3.0061	0.4839
hsa-miR-631	4.3710	2.9772	2.6277	0.4839
hsa-miR-487b	2.2864	0.5419	3.3507	0.8249
hsa-miR-543	1.4302	0.1764	2.3847	0.8249
hsa-miR-365	6.3121	5.3710	1.9200	0.8249
hsa-let-7e	6.8754	5.9369	1.9166	0.8249
hsa-miR-151-3p	3.8653	2.8896	1.9666	0.8249
hsa-miR-106b	6.7077	5.7538	1.9371	0.8249
hsa-miR-301a	4.3942	3.3753	2.0263	0.8249
hsa-miR-382	2.2284	0.8661	2.5709	0.8249
hsa-miR-100	4.7280	3.4939	2.3523	0.8249
hsa-miR-452	2.3510	1.1210	2.3456	0.8249
hsa-miR-371-5p	2.2495	1.1375	2.1614	0.8249
hsa-miR-765	4.3601	3.6031	1.6900	0.8249
hsa-miR-362-3p	2.5044	1.5707	1.9102	0.8249
hsa-miR-183	1.8260	0.5658	2.3953	0.8249
hsa-miR-423-5p	3.8130	3.0448	1.7032	0.8249
hsa-miR-328	6.1455	5.1186	2.0377	0.8249
hsa-miR-595	4.4023	3.3593	2.0605	0.8249
hsa-miR-542-3p	2.8903	1.2498	3.1177	0.8249
hsa-miR-550	1.9877	1.2773	1.6363	0.8249
hsa-miR-634	2.1901	1.4710	1.6462	0.8249
hsa-miR-188-5p	4.1637	3.5119	1.5711	1.3079
hsa-miR-450a	2.6452	1.0431	3.0358	1.3079
hsa-miR-181c	2.7493	1.7464	2.0040	1.3079
hsa-miR-126	8.1419	7.2671	1.8338	1.3079
hsa-miR-484	3.8659	3.2581	1.5239	1.3079

(Continued on the following page)

Published OnlineFirst March 27, 2012; DOI: 10.1158/1078-0432.CCR-11-1078

Table 1. Upregulated miRNAs in colorectal cancer stromal tissue compared with normal stromal tissue (Cont'd)

Systematic name	Signal in cancer stromal tissue (log_2)	Signal in normal stromal tissue (log_2)	Fold change	*Q* (%)
hsa-miR-95	2.2341	1.4163	1.7627	1.3079
hsa-miR-19a	7.0755	6.2318	1.7946	1.3079
hsa-miR-181a	6.7619	5.9594	1.7441	1.3079
hsa-miR-376a	4.3021	3.2870	2.0211	1.3079
hsa-miR-425	4.4042	3.5379	1.8230	1.3079
hsa-miR-455-5p	1.9466	0.6533	2.4510	1.3079
hsa-miR-324-3p	5.1796	4.5422	1.5555	1.3079
hsa-miR-622	2.5718	1.6357	1.9133	1.3079
hsa-miR-613	1.6581	0.9437	1.6408	1.3079
hsa-miR-575	3.9488	3.2521	1.6208	1.3079
hsa-miR-222	3.2655	2.5148	1.6827	1.3079
hsa-miR-32	2.5684	1.6119	1.9406	1.3079
hsa-miR-197	7.9098	7.0983	1.7551	1.3079
hsa-miR-766	6.9197	6.0107	1.8777	1.3079
hsa-miR-876-5p	1.3810	0.6503	1.6595	1.9848
hsa-miR-505	2.8023	2.0524	1.6817	1.9848
hsa-let-7c	7.3815	6.6304	1.6831	1.9848
hsa-miR-98	4.5308	3.7445	1.7247	1.9848
hsa-miR-27a	9.1504	8.3246	1.7725	1.9848
hsa-miR-324-5p	4.1229	3.2487	1.8330	1.9848
hsa-miR-874	3.6715	3.0471	1.5416	1.9848
hsa-miR-133a	1.3162	0.6960	1.5371	1.9848

NOTE: miRNAs which are components of miR-17-92a cluster or miR-25-106b cluster are marked (gray).

representative miRNAs from the 2 clusters, *miR-25*, and *miR-92a* in clinical samples. *MiR-25* and *miR-92a* are selected because of relative high expression in cancer stroma and because they have the same seed sequence and share the same targets and could work coordinately. In samples of normal epithelial tissue ($n = 4$), cancer epithelial tissue ($n = 10$), normal stromal tissue ($n = 4$), and cancer stromal tissue ($n = 26$), which included 13 cancer samples and 4

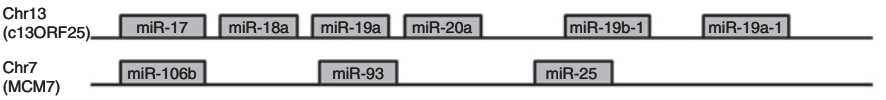

		Sequence	Seed pattern
17-92a cluster	hsa-miR-17	GAUGGACGUGACAUUCGUGAAAC	■
	hsa-miR-18a	GAUAGACGUGAUCUACGUGGAAU	◆
	hsa-miR-19a	AGUCAAAACGUAUCUAAACGUGU	●
	hsa-miR-20a	GAUGGACGUGAUAUUCGUGAAAU	■
	hsa-miR-19b	AGUCAAAACGUACCUAAACGUGU	●
	hsa-miR-92a	UGUCCGGCCCUGUUCACGUUAU	▲
25-106b cluster	hsa-miR-106b	UAGACGUGACAGUCGUGAAAU	■
	hsa-miR-25	AGUCUGGCUCUGUUCACGUUAC	▲
	hsa-miR-93	GAUGGACGUGCUUGUCGUGAAAC	■

Chr, chromosome

Figure 1. Top, schematic diagram showing the genomic structures of the 2 miRNA clusters located on chromosomes 13 and 7. The *miR-17-92a* cluster is located in the intron of host gene *C13ORF25* and *miR-25-106b* is in *MCM7*. Bottom, sequences of 2 miRNA cluster components. The same marks indicate seed sequence (2–8 mer from the 5′side) homology between the individual miRNAs.

Published OnlineFirst March 27, 2012; DOI: 10.1158/1078-0432.CCR-11-1078

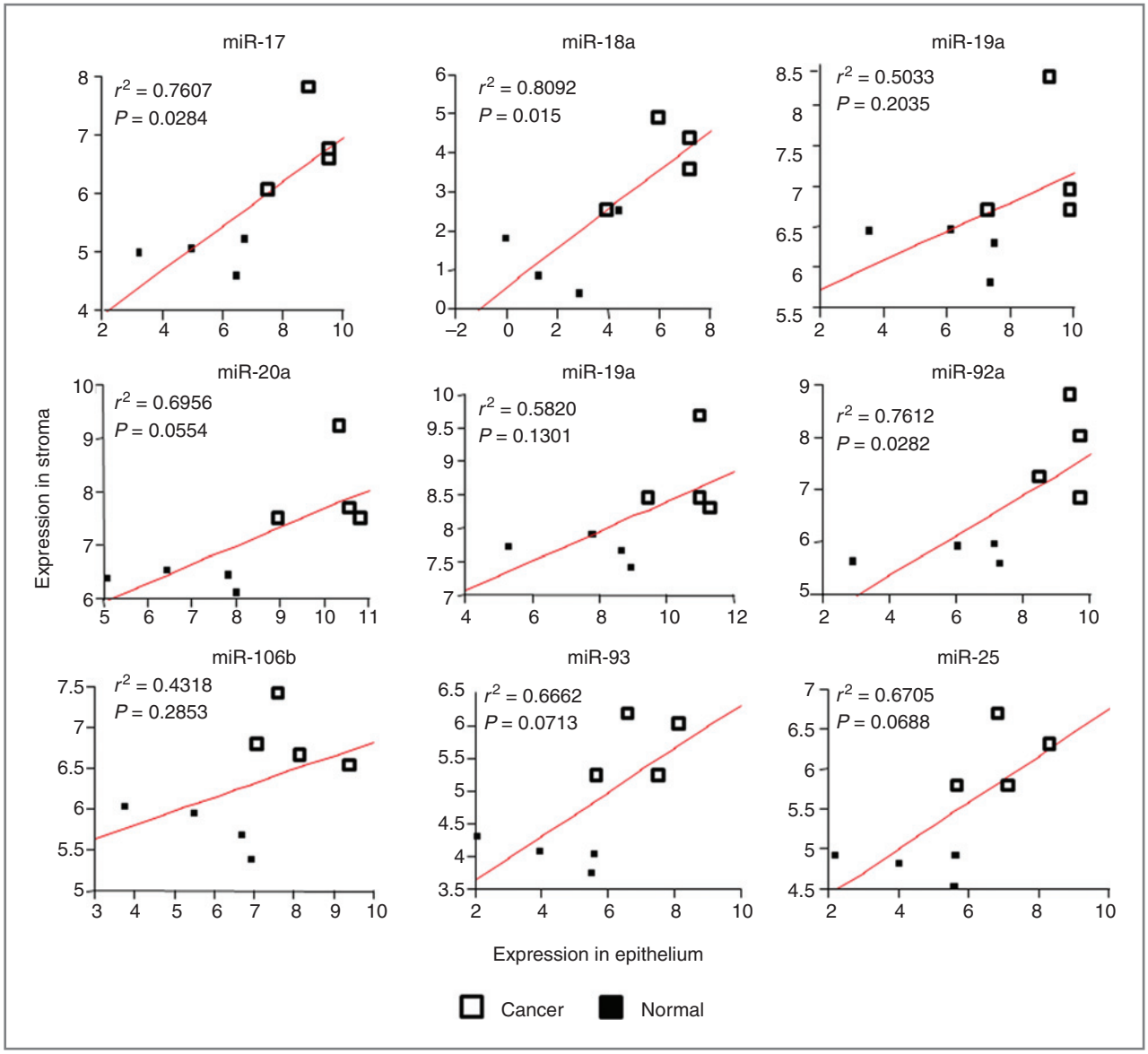

Figure 2. Correlation between the expression status of epithelial tissue and stromal tissue of *miR-17-92a* and *miR-25-106b* clusters. In all components of the clusters, expression status of the epithelial tissues and the stromal tissues was highly correlated and expression was higher in epithelium than in stroma.

normal samples used for microarray analysis, we carried out qRT-PCR to investigate the expression of *miR-25* and *miR-92a*. The data confirmed the upregulation of these miRNAs in cancer stroma compared with normal stroma in accordance with upregulation in cancer epithelium (Fig. 3).

miR-25 and miR-92a expression in colorectal cancer stroma was associated with clinicopathologic factors

For the 26 colorectal cancer stromal samples for which we used RT-PCR analysis, clinicopathologic data were available in 24 cases. Clinicopathologic analysis revealed that the high *miR-25* expression group (values > the 0.25 quartile; 0.54, normalized to RNU6B) had more advanced venous invasion compared with the low expression group (values < the 0.25 quartile; $P = 0.046$, Table 4). In the high *miR-92a* expression group (values > the 0.75 quartile; 1.16, normalized to RNU6B), there was greater lymphatic invasion ($P = 0.005$), venous invasion ($P = 0.016$), and liver metastasis ($P = 0.018$) compared with the low *miR-92a* expression group (values < the 0.75 quartile; Table 5). However, no significant differences were observed regarding age, gender, histology, lymphatic invasion, venous invasion, lymph node metastasis, peritoneal dissemination, or distant metastasis.

Downregulated miRNAs in colorectal cancer stromal tissue compared with normal stromal tissue

We also investigated downregulated miRNAs in cancer stroma compared with normal stroma. As a result,

Published OnlineFirst March 27, 2012; DOI: 10.1158/1078-0432.CCR-11-1078

Table 2. Genes downregulated in cancer stroma, which are putative targets of miR-17-92a and/or miR-25-106b clusters

Gene symbol	Genbank accession	Description	Fold Change[a]	*Q* (%)[a]	miR-17/20a/106b/93 target[b]	miR-18a target[b]	miR-19a/19b target[b]	miR-92a/25 target[b]
KEGG 04061: Cytokine–cytokine receptor interaction (chemokines, hematopoietins, PDGF family, TNF family, and TGFβ family)								
IL10RA	NM_001558	*Homo sapiens* interleukin 10 receptor, α (IL10RA)	0.2492	0.0000	○	○	○	
TNFRSF17	NM_001192	*Homo sapiens* TNF receptor superfamily, member 17 (TNFRSF17)	0.1313	0.0000	○	○		
LIFR	NM_002310	*Homo sapiens* leukemia inhibitory factor receptor alpha (LIFR)	0.1563	0.0000	○	○	○	
CXCL12	NM_199168	*Homo sapiens* chemokine (C-X-C motif) ligand 12 (stromal cell–derived factor 1; CXCL12), transcript variant 1	0.1218	0.0000			○	
BMP2	NM_001200	*Homo sapiens* bone morphogenetic protein 2 (BMP2)	0.1734	0.0748	○	○		
CNTFR	NM_147164	*Homo sapiens* ciliary neurotrophic factor receptor (CNTFR), transcript variant 1	0.2142	0.0748			○	
IL6R	NM_000565	*Homo sapiens* interleukin 6 receptor (IL6R), transcript variant 1	0.2694	0.0748	○	○		
PDGFRA	BC015186	*Homo sapiens* platelet-derived growth factor receptor, α polypeptide, mRNA (cDNA clone IMAGE: 4043984), complete cds.	0.2247	0.1256	○			○
TNFRSF13B	NM_012452	*Homo sapiens* TNF receptor superfamily, member 13B (TNFRSF13B)	0.2033	0.1256				○
XCL1	NM_002995	*Homo sapiens* chemokine (C motif) ligand 1 (XCL1)	0.1676	0.1256	○	○	○	○
CTF1	NM_001330	*Homo sapiens* cardiotrophin 1 (CTF1)	0.3178	0.2025		○		
XCL2	NM_003175	*Homo sapiens* chemokine (C motif) ligand 2 (XCL2)	0.2028	0.2025	○	○	○	
CCR9	NM_006641	*Homo sapiens* chemokine (C-C motif) receptor 9 (CCR9), transcript variant B	0.2514	0.2025	○	○	○	○
TGFBR2	NM_003242	*Homo sapiens* TGF, β receptor II (70/80 kDa) (TGFBR2), transcript variant 2	0.3819	0.3097	○		○	
CCL16	NM_004590	*Homo sapiens* chemokine (C-C motif) ligand 16 (CCL16)	0.3502	0.4833				○
IFNA2	NM_000605	*Homo sapiens* IFN, α 2 (IFNA2)	0.4167	0.7799		○	○	
GHR	NM_000163	*Homo sapiens* growth hormone receptor (GHR)	0.3538	0.7799			○	○
IFNW1	NM_002177	*Homo sapiens* IFN, omega 1 (IFNW1)	0.3926	0.7799			○	
IL15	NM_172174	*Homo sapiens* interleukin 15 (IL15), transcript variant 1	0.4331	0.7799				○
LEP	NM_000230	*Homo sapiens* leptin (obesity homolog, mouse; LEP)	0.3591	0.7799	○			
BMPR1B	NM_001203	*Homo sapiens* bone morphogenetic protein receptor, type IB (BMPR1B)	0.4251	1.2419	○	○		
FASLG	NM_000639	*Homo sapiens* Fas ligand (TNF superfamily, member 6; FASLG)	0.4284	1.2419	○	○	○	○

(Continued on the following page)

Published OnlineFirst March 27, 2012; DOI: 10.1158/1078-0432.CCR-11-1078

Table 2. Genes downregulated in cancer stroma, which are putative targets of miR-17-92a and/or miR-25-106b clusters (Cont'd)

Gene symbol	Genbank accession	Description	Fold Change[a]	*Q* (%)[a]	miR-17/20a/ 106b/93 target[b]	miR-18a target[b]	miR-19a/ 19b target[b]	miR-92a/25 target[b]
CCL13	NM_005408	*Homo sapiens* chemokine (C-C motif) ligand 13 (CCL13)	0.2404	1.2419				○
CCL5	NM_002985	*Homo sapiens* chemokine (C-C motif) ligand 5 (CCL5)	0.3839	1.2419	○	○	○	
IL9R	NM_176786	*Homo sapiens* interleukin 9 receptor (IL9R), transcript variant 2	0.4804	1.2419		○		
IL18R1	NM_003855	*Homo sapiens* interleukin 18 receptor 1 (IL18R1)	0.4667	1.2419			○	
IL29	NM_172140	*Homo sapiens* interleukin 29 (IFN, lambda 1; IL29)	0.4156	2.2195		○		
TNFRSF19	NM_018647	*Homo sapiens* TNF receptor superfamily, member 19 (TNFRSF19), transcript variant 1	0.4843	2.2195			○	
TSLP	NM_033035	*Homo sapiens* thymic stromal lymphopoietin (TSLP), transcript variant 1	0.3841	2.2195			○	
IL25	NM_022789	*Homo sapiens* interleukin 25 (IL25), transcript variant 1	0.4775	2.2195	○	○		
KEGG 04340 :Hedgehog signaling pathway								
WNT10A	NM_025216	*Homo sapiens* wingless type MMTV integration site family, member 10A (WNT10A)	0.1264	0.0000			○	
BMP2	NM_001200	*Homo sapiens* bone morphogenetic protein 2 (BMP2)	0.1734	0.0748	○	○		
BMP6	NM_001718	*Homo sapiens* bone morphogenetic protein 6 (BMP6)	0.2097	0.2025			○	
BMP5	NM_021073	*Homo sapiens* bone morphogenetic protein 5 (BMP5)	0.1747	0.3097				○
WNT9A	NM_003395	*Homo sapiens* wingless-type MMTV integration site family, member 9A (WNT9A)	0.3830	0.7799			○	
WNT1	NM_005430	*Homo sapiens* wingless-type MMTV integration site family, member 1 (WNT1)	0.4226	0.7799			○	
CSNK1A1	AF447582	*Homo sapiens* HLCDGP1 mRNA, complete cds.	0.4952	1.2419			○	
WNT7B	NM_058238	*Homo sapiens* wingless-type MMTV integration site family, member 7B (WNT7B)	0.4704	1.2419	○	○	○	
BMP8A	NM_181809	*Homo sapiens* bone morphogenetic protein 8a (BMP8A)	0.3596	2.2195				○
HHIP	AK074711	*Homo sapiens* cDNA FLJ90230 fis, clone NT2RM2000410	0.4494	3.4908				○
KEGG 05200 :Pathways in cancer								
CASP8	NM_033356	*Homo sapiens* caspase 8, apoptosis-related cysteine peptidase (CASP8), transcript variant C	0.1313	0.0000	○		○	
COL4A4	NM_000092	*Homo sapiens* collagen, type IV, alpha 4 (COL4A4)	0.0790	0.0000	○	○		
WNT10A	NM_025216	*Homo sapiens* wingless-type MMTV integration site family, member 10A (WNT10A)	0.1264	0.0000			○	
BCL2	NM_000633	*Homo sapiens* B-cell CLL/ lymphoma 2 (BCL2), nuclear gene encoding mitochondrial protein, transcript variant α	0.2490	0.0353	○			○

(Continued on the following page)

Published OnlineFirst March 27, 2012; DOI: 10.1158/1078-0432.CCR-11-1078

Table 2. Genes downregulated in cancer stroma, which are putative targets of miR-17-92a and/or miR-25-106b clusters (Cont'd)

Gene symbol	Genbank accession	Description	Fold Change[a]	*Q* (%)[a]	miR-17/20a/106b/93 target[b]	miR-18a target[b]	miR-19a/19b target[b]	miR-92a/25 target[b]
RASSF5	NM_182664	*Homo sapiens* Ras association (RalGDS/AF-6) domain family 5 (RASSF5), transcript variant 2	0.2031	0.0353			○	
BMP2	NM_001200	*Homo sapiens* bone morphogenetic protein 2 (BMP2)	0.1734	0.0748	○	○		
VHL	AF088066	*Homo sapiens* full-length insert cDNA clone ZD86C03.	0.3146	0.0748	○	○		
PDGFRA	BC015186	*Homo sapiens* platelet-derived growth factor receptor, α polypeptide, mRNA (cDNA clone IMAGE:4043984), complete cds	0.2247	0.1256	○			○
IGF1	NM_000618	*Homo sapiens* insulin-like growth factor 1 (somatomedin C; IGF1)	0.2991	0.2025		○	○	
ETS1	NM_005238	*Homo sapiens* v-ets erythroblastosis virus E26 oncogene homolog 1 (avian; ETS1)	0.3762	0.3097			○	○
TGFBR2	NM_003242	*Homo sapiens* TGF, β receptor II (70/80 kDa) (TGFBR2), transcript variant 2	0.3819	0.3097	○		○	
NKX3-1	NM_006167	*Homo sapiens* NK3 transcription factor related, locus 1 (*Drosophila*; NKX3-1)	0.4231	0.4833	○			
CBL	NM_005188	*Homo sapiens* Cas-Br-M (murine) ecotropic retroviral transforming sequence (CBL)	0.4498	0.4833		○	○	○
STK4	BC005231	*Homo sapiens* serine/threonine kinase 4, mRNA (cDNA clone IMAGE:3950315), complete cds.	0.4024	0.4833	○	○	○	
SMAD2	NM_005901	*Homo sapiens* SMAD family member 2 (SMAD2), transcript variant 1	0.3846	0.4833		○	○	○
FGFR2	NM_022970	*Homo sapiens* fibroblast growth factor receptor 2 (bacteria-expressed kinase, keratinocyte growth factor receptor, craniofacial dysostosis 1, Crouzon syndrome, Pfeiffer syndrome, Jackson–Weiss syndrome; FGFR2), transcript variant 2, mRNA	0.3038	0.4833			○	○
WNT9A	NM_003395	*Homo sapiens* wingless-type MMTV integration site family, member 9A (WNT9A)	0.3830	0.7799			○	
WNT1	NM_005430	*Homo sapiens* wingless-type MMTV integration site family, member 1 (WNT1)	0.4226	0.7799			○	
COL4A6	NM_033641	*Homo sapiens* collagen, type IV, α 6 (COL4A6), transcript variant B	0.1932	0.7799				○
PIK3CD	NM_005026	*Homo sapiens* phosphoinositide-3-kinase, catalytic, delta polypeptide (PIK3CD)	0.4580	0.7799				○
DAPK2	NM_014326	*Homo sapiens* death-associated protein kinase 2 (DAPK2)	0.3810	0.7799	○	○		○
FGF6	NM_020996	*Homo sapiens* fibroblast growth factor 6 (FGF6)	0.3913	0.7799			○	

(Continued on the following page)

Published OnlineFirst March 27, 2012; DOI: 10.1158/1078-0432.CCR-11-1078

Table 2. Genes downregulated in cancer stroma, which are putative targets of miR-17-92a and/or miR-25-106b clusters (Cont'd)

Gene symbol	Genbank accession	Description	Fold Change[a]	*Q* (%)[a]	miR-17/20a/ 106b/93 target[b]	miR-18a target[b]	miR-19a/ 19b target[b]	miR-92a/25 target[b]
PLD1	NM_002662	*Homo sapiens* phospholipase D1, phosphatidylcholine specific (PLD1)	0.4685	0.7799	○	○	○	
FASLG	NM_000639	*Homo sapiens* Fas ligand (TNF superfamily, member 6; FASLG)	0.4284	1.2419	○	○	○	○
RUNX1	X90978	*Homo sapiens* mRNA for an acute myeloid leukaemia protein (1,793 bp)	0.4519	1.2419	○	○		
SMAD3	U68019	*Homo sapiens* mad protein homolog (hMAD-3) mRNA, complete cds	0.4943	1.2419		○		
LAMA3	NM_000227	*Homo sapiens* laminin, alpha 3 (LAMA3), transcript variant 2	0.4329	1.2419	○			
DCC	NM_005215	*Homo sapiens* deleted in colorectal carcinoma (DCC)	0.4342	1.2419			○	
WNT7B	NM_058238	*Homo sapiens* wingless-type MMTV integration site family, member 7B (WNT7B)	0.4704	1.2419	○	○	○	
FGF5	NM_004464	*Homo sapiens* fibroblast growth factor 5 (FGF5), transcript variant 1	0.4823	2.2195	○			○
HHIP	AK074711	*Homo sapiens* cDNA FLJ90230 fis, clone NT2RM2000410.	0.4494	3.4908				○
KEGG 04514 :Cell adhesion molecules (CAM)								
CNTN2	NM_005076	*Homo sapiens* contactin 2 (axonal; CNTN2)	0.1659	0.0748	○	○	○	
ALCAM	NM_001627	*Homo sapiens* activated leukocyte cell adhesion molecule (ALCAM)	0.2975	0.1256		○		
CD22	NM_001771	*Homo sapiens* CD22 molecule (CD22)	0.1359	0.1256			○	
SPN	NM_001030288	*Homo sapiens* sialophorin (leukosialin, CD43; SPN), transcript variant 1	0.3110	0.2025	○	○		○
CLDN18	NM_016369	*Homo sapiens* claudin 18 (CLDN18), transcript variant 1	0.3400	0.2025	○	○		
CNTNAP2	NM_014141	*Homo sapiens* contactin-associated protein-like 2 (CNTNAP2)	0.3082	0.3097	○			○
CLDN19	NM_148960	*Homo sapiens* claudin 19 (CLDN19)	0.3840	0.4833	○	○	○	○
PTPRC	NM_002838	*Homo sapiens* protein tyrosine phosphatase, receptor type, C (PTPRC), transcript variant 1	0.3629	0.7799				○
NRXN1	NM_004801	*Homo sapiens* neurexin 1 (NRXN1), transcript variant alpha	0.3674	0.7799		○		
CD8A	NM_001768	*Homo sapiens* CD8a molecule (CD8A), transcript variant 1	0.4033	1.2419		○		
CLDN16	NM_006580	*Homo sapiens* claudin 16 (CLDN16)	0.4543	1.2419		○		
CNTNAP1	NM_003632	*Homo sapiens* contactin-associated protein 1 (CNTNAP1)	0.4725	1.2419		○		
NCAM1	NM_000615	*Homo sapiens* neural cell adhesion molecule 1 (NCAM1), transcript variant 1	0.4247	1.2419			○	
CD28	NM_006139	*Homo sapiens* CD28 molecule (CD28)	0.4997	2.2195	○	○	○	

(Continued on the following page)

Published OnlineFirst March 27, 2012; DOI: 10.1158/1078-0432.CCR-11-1078

Table 2. Genes downregulated in cancer stroma, which are putative targets of miR-17-92a and/or miR-25-106b clusters (Cont'd)

Gene symbol	Genbank accession	Description	Fold Change[a]	*Q* (%)[a]	miR-17/20a/106b/93 target[b]	miR-18a target[b]	miR-19a/19b target[b]	miR-92a/25 target[b]
L1CAM	NM_000425	*Homo sapiens* L1 cell adhesion molecule (L1CAM), transcript variant 1	0.4938	3.4908	○	○	○	
WNT9A	NM_003395	*Homo sapiens* wingless-type MMTV integration site family, member 9A (WNT9A)	0.3830	0.7799			○	
WNT1	NM_005430	*Homo sapiens* wingless-type MMTV integration site family, member 1 (WNT1)	0.4226	0.7799			○	
COL4A6	NM_033641	*Homo sapiens* collagen, type IV, alpha 6 (COL4A6), transcript variant B	0.1932	0.7799				○
PIK3CD	NM_005026	*Homo sapiens* phosphoinositide-3-kinase, catalytic, delta polypeptide (PIK3CD)	0.4580	0.7799				○
DAPK2	NM_014326	*Homo sapiens* death-associated protein kinase 2 (DAPK2)	0.3810	0.7799	○	○		○
FGF6	NM_020996	*Homo sapiens* fibroblast growth factor 6 (FGF6)	0.3913	0.7799			○	
PLD1	NM_002662	*Homo sapiens* phospholipase D1, phosphatidylcholine-specific (PLD1)	0.4685	0.7799	○	○	○	
FASLG	NM_000639	*Homo sapiens* Fas ligand (TNF superfamily, member 6; FASLG)	0.4284	1.2419	○	○	○	○
RUNX1	X90978	*Homo sapiens* mRNA for an acute myeloid leukaemia protein (1,793 bp).	0.4519	1.2419	○	○		
SMAD3	U68019	*Homo sapiens* mad protein homolog (hMAD-3)	0.4943	1.2419		○		
LAMA3	NM_000227	*Homo sapiens* laminin, alpha 3 (LAMA3), transcript variant 2	0.4329	1.2419	○			
DCC	NM_005215	*Homo sapiens* deleted in colorectal carcinoma (DCC)	0.4342	1.2419			○	
WNT7B	NM_058238	*Homo sapiens* wingless-type MMTV integration site family, member 7B (WNT7B)	0.4704	1.2419	○	○	○	
FGF5	NM_004464	*Homo sapiens* fibroblast growth factor 5 (FGF5), transcript variant 1	0.4823	2.2195	○			○
HHIP	AK074711	*Homo sapiens* cDNA FLJ90230 fis, clone NT2RM2000410.	0.4494	3.4908				○

NOTE: KEGG (ref. 18).

[a]Fold change < 0.50, *Q* < 0.05

[b]Based on the computational analysis by TargetScan (ref. 19, 20). Genes which are targets of each miRNA are marked with circle.

previously reported tumor-suppressive miRNAs, such as the *miR-192-miR-194* cluster, *miR-215*, *miR-29c*, *miR-26b*, and *let-7g* were all downregulated in cancer stromal tissues compared with normal stromal tissues (Supplementary Table S3) (22, 23). Downregulation of tumor-suppressive miRNAs in cancer stroma as well as upregulation of oncogenic miRNAs in cancer stroma indicated that alterations of miRNA expression in stromal tissues are similar to that in epithelial tissues.

Comparison of miRNA expression status in cancer stroma and cancer epithelium

Significantly upregulated or downregulated miRNAs in cancer stroma compared with cancer epithelium are listed in Supplementary Table S4A and S4B.

Discussion

In this study, we analyzed expression levels of miRNAs expressed in cancer stroma and revealed that many

Published OnlineFirst March 27, 2012; DOI: 10.1158/1078-0432.CCR-11-1078

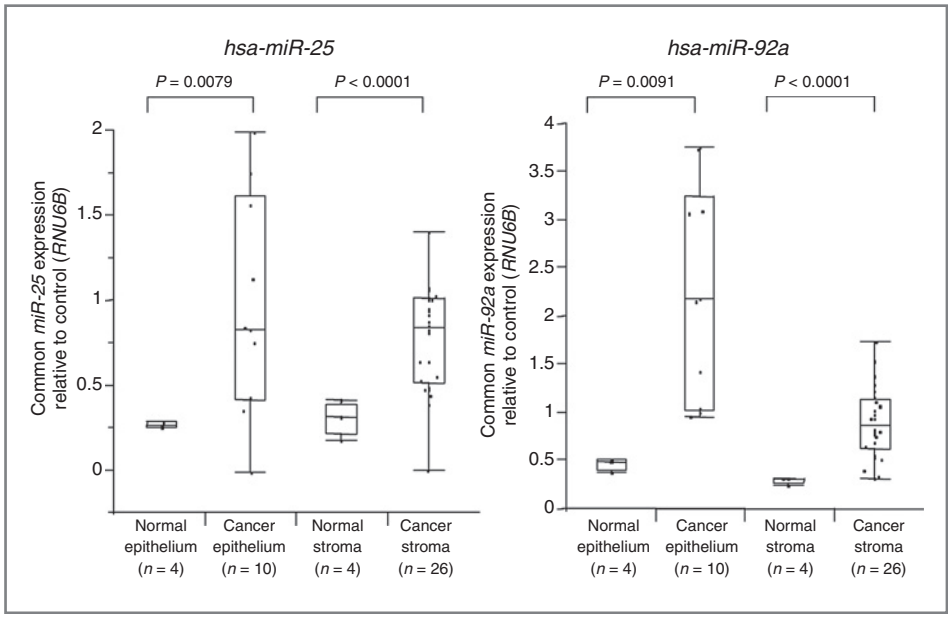

Figure 3. Expression of *miR-25* (left) and *miR-92a* (right) analyzed by quantitative RT-PCR in epithelium and stroma of cancer and normal tissue. Dots, expression of each sample; horizontal line, median; box, 25th through 75th percentile; error bars, range. Normal epithelium: $n = 4$, cancer epithelium: $n = 10$, normal stroma: $n = 4$, cancer stroma: $n = 26$.

oncogenic miRNAs including *miR-21* (24), *miR-221* (25), and almost all components of the *miR-17-92a* cluster and its homolog, and the *miR-106b-25* cluster were upregulated in cancer stroma compared with normal stroma (Table 1). Previous reports showed that the *miR-17-92a* cluster is upregulated in lung cancer, colorectal cancer, lymphoma, multiple myeloma, and medulloblastoma, whereas the *miR-106b-25* cluster is upregulated in gastric, colon, and prostate cancer, neuroblastoma, and multiple myeloma (9, 26, 27). Importantly, the expression of these miRNAs in stromal tissues had not been explored. We focused on these well-characterized miRNAs which are upregulated in cancer stroma as well as epithelial tissues.

The reason for the upregulation of such oncogenic miRNAs in stromal tissue is still unclear. However, previous studies have revealed genetic alterations such as LOH of cancer stromal cells (28) or epigenetic modification of cancer-associated fibroblasts (CAF; ref. 29). Hence, genetic or epigenetic changes of cancer stromal cells could be one explanation for this, although it remains controversial. Another possibility is intercellular transfer or penetration of miRNAs. It has been shown that secreted miRNAs from donor cells are transferred to and function in recipient cells. Some reports have shown that miRNAs are transferred in exosomes, vesicles of endocytic origin (30). If this occurred between cancer cells and stromal cells, profiles of miRNAs could become similar in both. We revealed that oncogenic miRNAs such as *miR-135b*, *miR-221*, and the *miR-17-92a* cluster were expressed at relatively higher levels in cancer epithelium than in stroma (Supplementary Table S4B). These findings suggest that upregulation of such oncogenic miRNAs in cancer stroma follows the upregulation of oncogenic miRNA in epithelium during carcinogenesis and cancer progression. However, further studies are required to confirm the interaction between cancer and its stroma.

Recently, Mestdagh and colleagues reported that the *miR-17-92* miRNA cluster regulated key components of the TGFβ pathway such as *SMAD2*, *SMAD4*, and *TGFBR2* in neuroblastoma (31). With regard to epithelial–mesenchymal interactions, Bhowmick and colleagues showed that ablation of *TGFBR2* in stromal tissue can lead to carcinogenesis and cancer progression *in vivo* (3). In our data, *TGFBR2*, *SMAD2*, and *SMAD3*, which are putative targets of the *miR-17-92a* and *miR-106b-25* cluster, were shown to be significantly repressed in cancer stroma (Table 2 and Table 3). These results suggest that, at least in part, inhibition of the TGFβ pathway in stromal tissue is associated with tumorigenesis and cancer progression. However, the putative miRNA target gene pathways we showed in this study have not been experimentally established, therefore, further exploration is needed to confirm that they function in stromal tissue.

Clinicopathologic analysis showed that miRNAs expression in stromal tissue is associated with the malignant potential of cancer (Table 4 and Table 5). High expression of *miR-25* was associated with venous invasion, and *miR-92a* with lymphatic and venous invasion and liver metastasis. These data indicate that miRNA expression in stroma as well as in the epithelium can influence tumor aggressiveness in colorectal cancer. Lymphatic or venous invasion occurs dominantly in stromal tissue; therefore these results are entirely reasonable. Although validation in a larger number of samples is required in future studies, our data indicate the potential clinical significance of miRNAs in cancer stroma.

Stromal tissues are constituted by various kinds of cells, including immune cells, endothelial cells, and fibroblasts. Previous reports suggested CAF or tumor-associated

Published OnlineFirst March 27, 2012; DOI: 10.1158/1078-0432.CCR-11-1078

Table 3. Highly inverse-correlated miRNA and putative target gene pairs

miRNA name	mRNA name	Genbank accession	Description	correlation coefficient[a]	*P*[a]	Pathway (KEGG)[b]
hsa-miR-17	ACPP	NM_001099	Acid phosphatase, prostate	–0.8549	0.0002	00361: gamma-Hexachlorocyclohexane degradation, 00740: Riboflavin metabolism
hsa-miR-18a	HTR1D	NM_000864	5-Hydroxytryptamine (serotonin) receptor 1D	–0.8467	0.0003	04080: Neuroactive ligand–receptor interaction
hsa-miR-17	DAPK2	NM_014326	Death-associated protein kinase 2	–0.8073	0.0009	05200: Pathways in cancer, 05219: Bladder cancer
hsa-miR-17	LY75	NM_002349	Lymphocyte antigen 75	–0.8072	0.0009	
hsa-miR-17	TRIM7	NM_203297	Tripartite motif-containing 7	–0.7794	0.0017	
hsa-miR-19b	CASP7	NM_033338	Caspase 7, apoptosis-related cysteine peptidase	–0.7728	0.0020	04210: Apoptosis, 05010: Alzheimer's disease
hsa-miR-17	SHROOM1	NM_133456	shroom family member 1	–0.7553	0.0028	
hsa-miR-19a	PDE11A	NM_016953	Phosphodiesterase 11A	–0.7406	0.0038	00230: Purine metabolism
hsa-miR-20a	SYT13	NM_020826	Synaptotagmin XIII	–0.7385	0.0039	
hsa-miR-18a	PDE11A	NM_016953	Phosphodiesterase 11A	–0.7377	0.0040	00230: Purine metabolism
hsa-miR-18a	SLC18A1	NM_003053	Solute carrier family 18 (vesicular monoamine), member 1	–0.7342	0.0043	05012: Parkinson's disease
hsa-miR-19a	CLIC5	NM_016929	Chloride intracellular channel 5	–0.7231	0.0052	
hsa-miR-19a	ARFIP1	NM_001025595	ADP-ribosylation factor interacting protein 1	–0.7229	0.0052	
hsa-miR-19a	KCNV1	NM_014379	Potassium channel, subfamily V, member 1	–0.7190	0.0056	
hsa-miR-18a	MYO7B	BC035615	Myosin VIIB	–0.7151	0.0060	
hsa-miR-17	PKDREJ	NM_006071	Polycystic kidney disease (polycystin) and REJ homolog (sperm receptor for egg jelly homolog, sea urchin)	–0.7108	0.0065	
hsa-miR-19a	STX18	NM_016930	syntaxin 18	–0.7068	0.0069	04130: SNARE interactions in vesicular transport
hsa-miR-17	TRIM68	NM_018073	Tripartite motif-containing 68	–0.7058	0.0070	
hsa-miR-18a	SLC35D2	NM_007001	Solute carrier family 35, member D2	–0.7051	0.0071	
hsa-miR-17	TCF7	NM_003202	Transcription factor 7 (T-cell specific, HMG box)	–0.7023	0.0074	04310: Wnt signaling pathway, 04520: Adherens junction, 04916: Melanogenesis, 05200: Pathways in cancer, 05210: Colorectal cancer, 05213: Endometrial cancer, 05215: Prostate cancer, 05216: Thyroid cancer, 05217: Basal cell carcinoma, 05221: Acute myeloid leukemia, 05412: Arrhythmogenic right ventricular cardiomyopathy (ARVC)

(Continued on the following page)

Published OnlineFirst March 27, 2012; DOI: 10.1158/1078-0432.CCR-11-1078

Table 3. Highly inverse-correlated miRNA and putative target gene pairs (Cont'd)

miRNA name	mRNA name	Genbank accession	Description	correlation coefficient[a]	*P*[a]	Pathway (KEGG)[b]
hsa-miR-18a	SLC5A9	NM_001011547	Solute carrier family 5 (sodium/glucose cotransporter), member 9	–0.7009	0.0076	
hsa-miR-19a	ABLIM1	NM_001003408	Actin binding LIM protein 1	–0.6966	0.0082	04360: Axon guidance
hsa-miR-18a	CASP7	NM_033338	Caspase 7, apoptosis-related cysteine peptidase	–0.6960	0.0082	04210: Apoptosis, 05010: Alzheimer's disease
hsa-miR-20a	H2AFJ	NM_177925	H2A histone family, member J	–0.6939	0.0085	05322: Systemic lupus erythematosus
hsa-miR-17	SLC39A8	NM_022154	Solute carrier family 39 (zinc transporter), member 8	–0.6910	0.0089	
hsa-miR-17	CLIC5	NM_016929	Chloride intracellular channel 5	–0.6887	0.0092	
hsa-miR-20a	KIAA0319	NM_014809	KIAA0319	–0.6783	0.0108	
hsa-miR-19a	CEACAM8	NM_001816	Carcinoembryonic antigen-related cell adhesion molecule 8	–0.6751	0.0114	
hsa-miR-19a	TRIM68	NM_018073	Tripartite motif-containing 68	–0.6714	0.0120	
hsa-miR-19a	SFT2D3	NM_032740	SFT2 domain containing 3	–0.6684	0.0125	
hsa-miR-17	GGT6	NM_153338	γ-glutamyltransferase 6	–0.6676	0.0127	00430: Taurine and hypotaurine metabolism, 00450: Selenoamino acid metabolism, 00460: Cyanoamino acid metabolism, 00480: Glutathione metabolism, 00590: Arachidonic acid metabolism, 01100: Metabolic pathways
hsa-miR-20a	XDH	NM_000379	Xanthine dehydrogenase	–0.6673	0.0127	00230: Purine metabolism, 00232: Caffeine metabolism, 00983: Drug metabolism–other enzymes, 01100: Metabolic pathways
hsa-miR-20a	PPARA	NM_005036	Peroxisome proliferator-activated receptor α	–0.6654	0.0131	03320: PPAR signaling pathway, 04920: Adipocytokine signaling pathway
hsa-miR-17	C2orf15	NM_144706	Chromosome 2 open reading frame 15	–0.6653	0.0131	
hsa-miR-17	GK5	BX648681	Glycerol kinase 5 (putative)	–0.6634	0.0134	
hsa-miR-17	SIDT1	NM_017699	SID1 transmembrane family, member 1	–0.6619	0.0137	
hsa-miR-25	ATP10B	AB018258	ATPase, class V, type 10B	–0.6605	0.0140	
hsa-miR-17	TMC5	NM_024780	Transmembrane channel-like 5	–0.6590	0.0143	
hsa-miR-18a	ALDH1A2	NM_170697	Aldehyde dehydrogenase 1 family, member A2	–0.6586	0.0144	00830: Retinol metabolism, 01100: Metabolic pathways
hsa-miR-17	INADL	NM_176877	InaD-like (*Drosophila*)	–0.6516	0.0158	04530: Tight junction

NOTE: Based on the computational analysis by TargetScan (ref. 19, 20).

[a]Correlation coefficient <–0.65, $P < 0.05$ Ranked by correlation coefficient.

[b]KEGG, kyoto encyclopedia of genes and genomes (ref. 18).

Published OnlineFirst March 27, 2012; DOI: 10.1158/1078-0432.CCR-11-1078

Table 4. *miR-25* expression in cancer stroma and clinocopathologic factors

Factors	High expression ($n = 18$)	Low expression ($n = 6$)	*P*
Age (mean ± SD)	62.8 ± 2.95	66.5 ± 5.11	0.54
Sex			
Male	9	5	0.13
Female	9	1	
Histologic grade			
Well/moderately	11	4	0.81
Poorly/others	7	2	
Size			
50 mm≥ (small)	10	4	0.63
51 mm≤ (large)	8	2	
Depth of tumor invasion[a]			
m, sm, mp[a]	6	2	1
ss, se, si	12	4	
Lymph node metastasis			
Absent	13	2	0.092
Present	5	4	
Lymphatic invasion			
Absent	6	4	0.15
Present	12	2	
Venous invasion			
Absent	4	4	0.046[b]
Present	14	2	
Liver metastasis			
Absent	15	5	1
Present	3	1	
Dukes stage			
AB	11	2	0.24
CD	7	4	

[a]Tumor invasion of mucosa (m), submucosa (sm), muscularis propria (mp), subserosa (ss), penetration of serosa (se), and invasion of adjacent strucures (si)
[b]P < 0.05.

Table 5. *miR-92a* expression in cancer stroma and clinocopathologic factors

Factors	High expression ($n = 6$)	Low expression ($n = 18$)	*P*
Age (mean ± SD)	72.0 ± 4.74	61.0 ± 2.74	0.057
Sex			
Male	4	10	0.63
Female	2	8	
Histologic grade			
Well/moderately	4	11	0.81
Poorly/others	2	7	
Size			
50 mm> (small)	3	11	0.63
51 mm< (large)	3	7	
Depth of tumor invasion[a]			
m, sm, mp[a]	1	7	0.3
ss, se, si	5	11	
Lymph node metastasis			
Absent	3	12	0.47
Present	3	6	
Lymphatic invasion			
Absent	0	10	0.0050[b]
Present	6	8	
Venous invasion			
Absent	0	8	0.016[b]
Present	6	10	
Liver metastasis			
Absent	3	17	0.018[b]
Present	3	1	
Dukes stage			
AB	2	11	0.24
CD	4	7	

[a]Tumor invasion of mucosa (m), submucosa (sm), muscularis propria (mp), subserosa (ss), penetration of serosa (se), and invasion of adjacent strucures (si).
[b]*P* < 0.05.

macrophage could enhance tumor progression and metastasis (4, 32), and Vermeulen and colleagues showed that myofibroblasts play a role in the maintenance of cancer stem cell properties (33). In this study, we analyzed unsorted samples of stromal tissue, therefore the miRNA profiling for each cell type was not available. Sorting according to surface antigen, such as CD31 for endothelial cells or CD14 for macrophage, will be required for cell type–specific investigations in future studies.

Our findings suggest the possibility that oncogenic miRNAs including the *miR-17-92a* and *miR-25-106b* clusters in colorectal cancer stromal tissues are functionally associated with cancer progression. Because our results are based on microarray data derived from a small sample size, further validation is required.

Disclosure of Potential Conflicts of Interest

No potential conflicts of interest were disclosed.

Authors' Contributions

Conception and design: N. Nishida, M. Nagahara, K. Mimori, H. Ishii, M. Mori
Development of methodology: N. Nishida, M. Nagahara, F. Tanaka, H. Ishii, M. Mori
Acquisition of data (provided animals, acquired and managed patients, provided facilities, etc.): N. Nishida, H. Ishii, M. Mori
Analysis and interpretation of data (e.g., statistical analysis, biostatistics, computational analysis): N. Nishida, T. Sato, H. Ishii, M. Mori
Writing, review, and/or revision of the manuscript: N. Nishida, K. Mimori, T. Sudo, F. Tanaka, H. Ishii, M. Mori
Administrative, technical, or material support (i.e., reporting or organizing data, constructing databases): N. Nishida, T. Sudo, H. Ishii, M. Mori
Study supervision: N. Nishida, K. Mimori, F. Tanaka, K. Shibata, K. Sugihara, Y. Doki, M. Mori

Published OnlineFirst March 27, 2012; DOI: 10.1158/1078-0432.CCR-11-1078

Acknowledgments

The authors thank T. Shimooka, K. Ogata, M. Kasagi, and T. Kawano for their excellent technical assistance.

Grant Support

This work was supported in part by the following grants and foundations: CREST, Japan Science and Technology Agency (JST); Japan Society for the Promotion of Science (JSPS) grant-in-aid for Scientific Research: 21679006, 20390360, 20590313, 20591547, 21591644, 21592014, 20790960, 21791297, 21229015, 20659209, and 20012039; NEDO (New Energy and Industrial Technology Development Organization) Technological Development for Chromosome Analysis; The Ministry of Education, Culture, Sports, Science and Technology of Japan for Scientific Research on Priority Areas, Cancer Translational Research Project, Japan; and LS094, Bureau of Science, Technology and Innovation Policy, Cabinet Office, Government Of Japan.

The costs of publication of this article were defrayed in part by the payment of page charges. This article must therefore be hereby marked *advertisement* in accordance with 18 U.S.C. Section 1734 solely to indicate this fact.

Received April 22, 2011; revised March 14, 2012; accepted March 15, 2012; published OnlineFirst March 27, 2012.

References

1. Kurose K, Gilley K, Matsumoto S, Watson PH, Zhou XP, Eng C. Frequent somatic mutations in PTEN and TP53 are mutually exclusive in the stroma of breast carcinomas. Nat Genet 2002;32:355–7.
2. Trimboli AJ, Cantemir-Stone CZ, Li F, Wallace JA, Merchant A, Creasap N, et al. Pten in stromal fibroblasts suppresses mammary epithelial tumours. Nature 2009;461:1084–91.
3. Bhowmick NA, Chytil A, Plieth D, Gorska AE, Dumont N, Shappell S, et al. TGF-beta signaling in fibroblasts modulates the oncogenic potential of adjacent epithelia. Science 2004;303:848–51.
4. Kalluri R, Zeisberg M. Fibroblasts in cancer. Nat Rev Cancer 2006;6:392–401.
5. Sund M, Kalluri R. Tumor stroma derived biomarkers in cancer. Cancer Metastasis Rev 2009;28:177–83.
6. Finak G, Bertos N, Pepin F, Sadekova S, Souleimanova M, Zhao H, et al. Stromal gene expression predicts clinical outcome in breast cancer. Nat Med 2008;14:518–27.
7. Fukino K, Shen L, Patocs A, Mutter GL, Eng C. Genomic instability within tumor stroma and clinicopathological characteristics of sporadic primary invasive breast carcinoma. JAMA 2007;297:2103–11.
8. Bartel DP. MicroRNAs: target recognition and regulatory functions. Cell 2009;136:215–33.
9. Nicoloso MS, Spizzo R, Shimizu M, Rossi S, Calin GA. MicroRNAs–the micro steering wheel of tumour metastases. Nat Rev Cancer 2009;9:293–302.
10. Nishida K, Mine S, Utsunomiya T, Inoue H, Okamoto M, Udagawa H, et al. Global analysis of altered gene expressions during the process of esophageal squamous cell carcinogenesis in the rat: a study combined with a laser microdissection and a cDNA microarray. Cancer Res 2005;65:401–9.
11. Wang H, Ach RA, Curry B. Direct and sensitive miRNA profiling from low-input total RNA. RNA 2007;13:151–9.
12. Quackenbush J. Microarray data normalization and transformation. Nat Genet 2002;32 Suppl:496–501.
13. Lopez-Romero P, Gonzalez MA, Callejas S, Dopazo A, Irizarry RA. Processing of Agilent microRNA array data. BMC Res Notes 2010;3:18.
14. Lopez-Romero P. Pre-processing and differential expression analysis of Agilent microRNA arrays using the AgiMicroRna Bioconductor library. BMC Genomics 2011;12:64.
15. Brazma A, Hingamp P, Quackenbush J, Sherlock G, Spellman P, Stoeckert C, et al. Minimum information about a microarray experiment (MIAME)-toward standards for microarray data. Nat Genet 2001;29:365–71.
16. Nogales-Cadenas R, Carmona-Saez P, Vazquez M, Vicente C, Yang X, Tirado F, et al. GeneCodis: interpreting gene lists through enrichment analysis and integration of diverse biological information. Nucleic Acids Res 2009;37:W317–22.
17. Carmona-Saez P, Chagoyen M, Tirado F, Carazo JM, Pascual-Montano A. GENECODIS: a web-based tool for finding significant concurrent annotations in gene lists. Genome Biol 2007;8:R3.
18. Kanehisa M, Goto S. KEGG: kyoto encyclopedia of genes and genomes. Nucleic Acids Res 2000;28:27–30.
19. Lewis BP, Burge CB, Bartel DP. Conserved seed pairing, often flanked by adenosines, indicates that thousands of human genes are microRNA targets. Cell 2005;120:15–20.
20. Grimson A, Farh KK, Johnston WK, Garrett-Engele P, Lim LP, Bartel DP. MicroRNA targeting specificity in mammals: determinants beyond seed pairing. Mol Cell 2007;27:91–105.
21. Olive V, Jiang I, He L. mir-17-92, a cluster of miRNAs in the midst of the cancer network. Int J Biochem Cell Biol 2010;42:1348–54.
22. Spizzo R, Nicoloso MS, Croce CM, Calin GA. SnapShot: MicroRNAs in cancer. Cell 2009;137:586–586.e1.
23. Braun CJ, Zhang X, Savelyeva I, Wolff S, Moll UM, Schepeler T, et al. p53-Responsive micrornas 192 and 215 are capable of inducing cell cycle arrest. Cancer Res 2008;68:10094–104.
24. Asangani IA, Rasheed SA, Nikolova DA, Leupold JH, Colburn NH, Post S, et al. MicroRNA-21 (miR-21) post-transcriptionally downregulates tumor suppressor Pdcd4 and stimulates invasion, intravasation and metastasis in colorectal cancer. Oncogene 2008;27:2128–36.
25. le Sage C, Nagel R, Egan DA, Schrier M, Mesman E, Mangiola A, et al. Regulation of the p27(Kip1) tumor suppressor by miR-221 and miR-222 promotes cancer cell proliferation. EMBO J 2007;26:3699–708.
26. Petrocca F, Visone R, Onelli MR, Shah MH, Nicoloso MS, de Martino I, et al. E2F1-regulated microRNAs impair TGFbeta-dependent cell-cycle arrest and apoptosis in gastric cancer. Cancer Cell 2008;13:272–86.
27. Ventura A, Young AG, Winslow MM, Lintault L, Meissner A, Erkeland SJ, et al. Targeted deletion reveals essential and overlapping functions of the miR-17 through 92 family of miRNA clusters. Cell 2008;132:875–86.
28. Allinen M, Beroukhim R, Cai L, Brennan C, Lahti-Domenici J, Huang H, et al. Molecular characterization of the tumor microenvironment in breast cancer. Cancer Cell 2004;6:17–32.
29. Hu M, Yao J, Cai L, Bachman KE, van den Brule F, Velculescu V, et al. Distinct epigenetic changes in the stromal cells of breast cancers. Nat Genet 2005;37:899–905.
30. Valadi H, Ekstrom K, Bossios A, Sjostrand M, Lee JJ, Lotvall JO. Exosome-mediated transfer of mRNAs and microRNAs is a novel mechanism of genetic exchange between cells. Nat Cell Biol 2007;9:654–9.
31. Mestdagh P, Bostrom AK, Impens F, Fredlund E, Van Peer G, De Antonellis P, et al. The miR-17-92 microRNA cluster regulates multiple components of the TGF-beta pathway in neuroblastoma. Mol Cell 2010;40:762–73.
32. Qian BZ, Pollard JW. Macrophage diversity enhances tumor progression and metastasis. Cell 2010;141:39–51.
33. Vermeulen L, De Sousa EMF, van der Heijden M, Cameron K, de Jong JH, Borovski T, et al. Wnt activity defines colon cancer stem cells and is regulated by the microenvironment. Nat Cell Biol 2010;12:468–76.

AACR American Association for Cancer Research

Clinical Cancer Research

Microarray Analysis of Colorectal Cancer Stromal Tissue Reveals Upregulation of Two Oncogenic miRNA Clusters

Naohiro Nishida, Makoto Nagahara, Tetsuya Sato, et al.

Clin Cancer Res Published OnlineFirst March 27, 2012.